Received: 2 December 2021 | Revised: 14 June 2022 | Accepted: 14 June 2022

DOI: 10.1002/joc.7764

RESEARCH ARTICLE

International Journal of Climatology RMetS

Wind wave footprint of tropical cyclones from satellite data

Laura Cagigal[1,2] | **Fernando J. Méndez**[2] | **Sara O. van Vloten**[2] | **Ana Rueda**[2] | **Giovanni Coco**[1]

[1]School of Environment, University of Auckland, Auckland, New Zealand

[2]Geomatics and Ocean Engineering Group, Departamento de Ciencias y Técnicas del Agua y del Medio Ambiente, E.T.S.I.C.C.P. Universidad de Cantabria, Santander, Spain

Correspondence
Laura Cagigal, School of Environment, University of Auckland, 23 Symonds Street, Auckland, New Zealand.
Email: cagigall@unican.es

Funding information
Ministerio de Ciencia e Innovación, Grant/Award Number: Beach4cast PID2019-107053RB-I00; U.S. Department of Defense, Grant/Award Number: SERDP RC-2644; University of Auckland; Juan de la Cierva Incorporación Scholarship, Grant/Award Number: IJC2020-04390

Abstract

Tropical cyclones are associated with extreme winds, waves, and storm surge, being among most destructive natural phenomena. Developing capability for a rapid impact estimate is crucial for coastal applications and risk preparedness. When predicting waves characteristics associated to tropical cyclones, the traditional approach involves a two-step procedure (a) a Holland-type wind vortex model and (b) numerical simulations using a wave generation model, using buoy and satellite measurements for validation. In this work, we take advantage of the increasing amount of remote sensing observational data and propose a new empirical model to estimate the wind wave footprint of tropical cyclones. For this purpose, we construct a dataset with over a million satellite observations of waves triggered by tropical cyclones assuming a circular shape of the TC influence area and defining composites of significant wave height as a function of representative parameters of the track characteristics like the minimum pressure, its forward velocity, and its latitude. The validation against buoy data confirms the usefulness of the model for a first and rapid estimation of the wave footprint, although an underestimation of the most extreme events is observed due to the relatively small number of observations recorded. Due to its efficiency, the model can be applied for rapid estimations of wave footprints in operational systems, reconstruction of historical or synthetic events and risk assessments.

KEYWORDS

clustering techniques, satellite data, self-organizing maps, tropical cyclones, wave footprint, wind waves

1 | INTRODUCTION

Tropical cyclones (TCs), also named hurricanes or typhoons, represent one of the most extreme and deadliest natural phenomena in the world. Waves generated by extreme winds related to the moving TC pose a great risk for exposed areas in terms of infrastructure destruction, beach erosion, or coastal flooding. Furthermore, although storm surge induced by tropical cyclones tends to be more concentrated and close to the cyclone centre, waves generated can propagate many kilometres away from the centre (Moon *et al.*, 2003; Walsh *et al.*, 2012) and cause severe flooding at distant locations (Hoeke *et al.*, 2021).

Waves generated by TCs are an extreme example of wind–wave interactions and their study is necessary to support risk assessments and mitigation efforts. These assessments are hampered by both the lack of extensive records of historical TCs (Bloemendaal *et al*., 2020) and the severe and complicated wave field generated by intense and fast-varying winds (Moon *et al*., 2003). Globally, a mean of about 90–100 TCs occurs annually (Bloemendaal *et al*., 2020; Hoogewind *et al*., 2020), with reliable datasets starting in 1980. Furthermore, the characteristics of tropical cyclones are expected to globally change over time due to climatic effects, with a poleward shift of TC tracks (Hemer *et al*., 2013; Daloz and Camargo, 2018; Hoogewind *et al*., 2020) and a gradual increase of tropical cyclone frequency and intensity (Emanuel, 2013). These changes will have a chain effect in extreme storm surge and wave climate at middle latitudes (Mori and Takemi, 2016).

Nevertheless, future projections of changes in TC activity are based on global climate models (GCMs) and rely on its ability to correctly represent TCs, as the potential cost of underpredicting its intensity could be enormous (Abdalla *et al*., 2021). Hodges *et al*. (2017) studied the representation of TCs in historical reanalysis datasets, concluding that although nearly all the historical TCs were represented, the wind intensities were significantly lower and pressures were too high, leading to wave and storm surge hindcast models not able of capturing extreme events (Cid *et al*., 2017; Cagigal *et al*., 2019). This underestimation, mostly due to a nonsufficient resolution of reanalysis models (Durrant *et al*., 2014; Hodges *et al*., 2017), provides evidence of the need of observations to calibrate numerical wave and storm surge models. In the case of TCs, sparse both in time and space, these observations can be acquired from the dense network of satellite information available worldwide.

With this increasing amount of remote and in situ measurements, the wind wave field generated by tropical cyclones, which was usually assumed to mirror the wind field, has been demonstrated to have a more complex spatial distribution (Young, 2017), with a pronounced asymmetry of the TC wave field (King and Shemdin, 1979; Young and Vinoth, 2013; Tamizi and Young, 2020; Ponce de León and Bettencourt, 2021). This asymmetry is primarily caused by the forward motion of the TC, causing waves to the right (left in southern regions) of the track to be exposed to the wind for a prolonged time causing a trapped-fetch effect (Bowyer and MacAfee, 2005).

Different models to predict the wind waves generated by TCs have been presented (Young and Vinoth, 2013; Young, 1988; 2017), mainly focusing on predicting the maximum significant wave height (SWH), although attempts to obtain the spatial SWH field from numerical modelling and measured data have also been made (Young, 2017; Tamizi and Young, 2020). To capture the spatial variability of wind wave TCs, a dense network of observations, especially for extreme conditions, is required (Tamizi and Young, 2020). For this reason, in the last few years, satellite information has been used to explore TC characteristics and extreme events (Knaff *et al*., 2014; Young, 2017; Takbash *et al*., 2019; Tamizi and Young, 2020), resulting in extreme value estimates consistent with buoy data (Takbash *et al*., 2019) without relying on in situ buoy measurements, which are sparse and known to fail when exposed to very extreme conditions.

This paper builds and analyses a database of wave conditions from satellite measurements associated to TCs worldwide. The objective is to combine a TC (Knapp *et al*., 2018) and an altimeter dataset (Ribal and Young, 2019), to obtain a database with over a thousand tropical cyclones with associated satellite waves. Such a unique dataset with more than 1 million of observations will be analysed and explored to understand and develop an estimate of the wind waves generated by TCs. The analysis will be based on the clustering technique of self-organizing maps (SOM) for an intuitive 2D lattice of the influence of the TC parameters on the wave footprint (Camus *et al*., 2011b).

We aim to generate a comprehensive dataset of satellite SWH observations triggered by TCs worldwide, and to use such a dataset to fit a predictive model. The paper is organized as follows. Section 2 presents the data sources used to build the database, whose construction is presented in section 3. Section 4 outlines the clustering of the SWH generated by TCs. Section 5 focuses on the applications and validation of the clustering technique for a preliminary estimate of the SWH footprint generated by any given track worldwide, while a discussion and concluding remarks are presented on section 6.

2 | DATA

2.1 | Tropical cyclone data

The database selected for the historical TCs is the International Best Track Achieve for Climate Stewardship (IBTrACS) version 4, first released in 2018 (Knapp *et al*., 2018). The database combines best track data from a number of meteorological centres worldwide, providing a homogenized global dataset with records from 1852. TCs information is combined considering the reports from the official World Meteorological Organization in charge of each region.

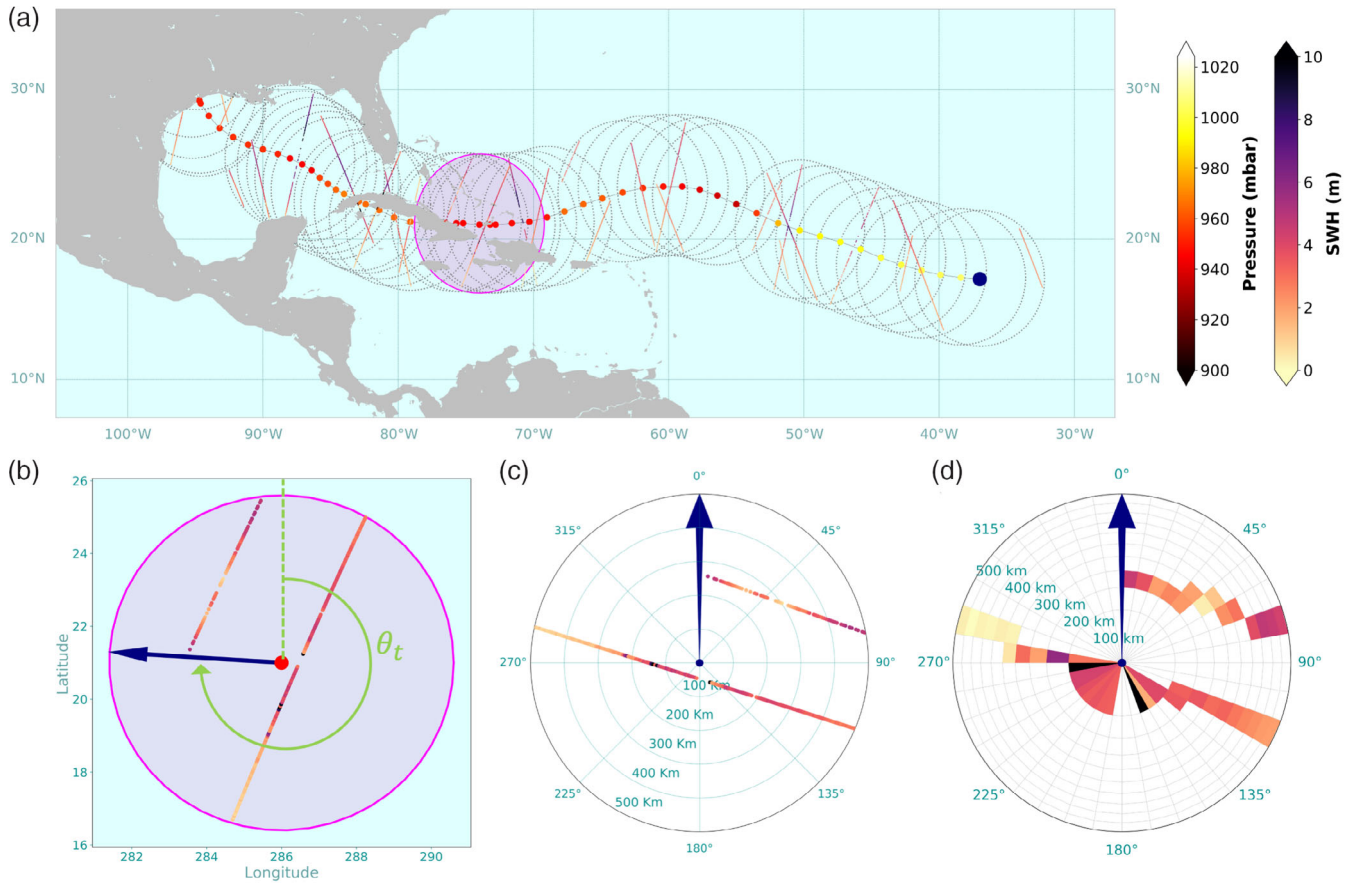

FIGURE 1 Methodology for generating the database. (a) TC track with associated SWH satellite measurements from IMOS in a 500-km radius from each point of the track, (b) selection of a point from the TC track with its associated SWH, highlighted in colour in panel (a). (c) SWH information in (b) reprojected to the new reference polar coordinated system. (d) SWH information from (b) translated to the congruent grid defined for the methodology [Colour figure can be viewed at wileyonlinelibrary.com]

2.2 | Wave data

Satellite wave data has been extracted from the Integrated Marine Observing System (IMOS) database (Ribal and Young, 2019), which consists of global SWH and wind speed from 13 altimeters starting in 1985. It provides the information for all the different altimeter missions under the same format, on a regular grid of 1° worldwide. IMOS database has been selected as it has been calibrated against buoy data from the National Oceanographic Data Center as well as cross-validated with altimeters to test for consistency. The database is updated every 6 months and data can easily be downloaded using a graphical interface.

The altimeter data provided by IMOS covers the period from 1985 to 2020, except for the lapse between 1990 and 1991 when no satellite missions were deployed. For the analysis provided in this paper, the whole database has been used, while a range of different filters to differentiate outliers from the database have been used during the development of the methodology.

In order to compare the results of the satellite derived analysis, an external source of data is needed. For this purpose, the National Buoy Data Center (NDBC) buoy network has been selected, using a total of 40 buoys located in deep waters around the United States.

3 | DATABASE DEVELOPMENT

Combining IMOS and IBTrACS allows to obtain the spatial distribution of waves associated to historical TCs worldwide. The aim is to generate a comprehensive database accounting for all the satellite data available over a time interval and over an influence radius centred at each point of the TC track. The methodology assumes a wave influence of circular shape with a 500-km radius at each point, and defines, in moving polar coordinates with respect to the forward direction, the maximum SWH within a time interval, which has been fixed to 3 hr as in Tamizi and Young (2020). Following previous studies,

radius has been fixed to 500 km in order to capture the nature of the waves propagating away from the TC eye (Kita *et al*., 2018; Tamizi and Young, 2020; Ponce de León and Bettencourt, 2021). The procedure to generate the database is exemplified for one historical TC in Figure 1. Figure 1a shows the track of the selected TC with its associated wave satellite data inside the influence area (grey circles) and time range at each point of the track. The coloured circle has been chosen to exemplify the transformation from the satellite wave data defined in position by [Lon, Lat] (Figure 1b) to the polar coordinated system referred to the translation direction as in Figure 1c.

This transformation allows to generalize the reference for all the TCs worldwide. We have chosen the Northern Hemisphere (NH) to be used as the reference for our composites, so that the waves from the Southern Hemisphere (SH) are flipped right–left. This transformation is done in order to take into account the clockwise wind direction in the NH, opposed to the anticlockwise rotation in the SH. This opposite rotation makes the waves generated by a tropical cyclone in the NH be larger in the forward right quadrant of the TC, while in the SH the forward left quadrant is the one accounting for the largest waves.

In order to discretise the data, we generate a congruent mesh (Beckers and Beckers, 2012) as the one in Figure 1d, discretised every 10° in radius, and compartmentalize in 10 variable distances, so that each of the cells has the same area to make sure that the amount of data that will fall into each cell is homogeneous. For each TC and point of the track, the maximum SWH of the data contained in each cell is stored for the analysis (Figure 1d).

Following this methodology and combining all the TCs with information of minimum pressure worldwide with the satellite waves from IMOS, results in a database with ∼37,000 track points which have at least one cell with wave data, and almost a million cells with wave information in total, corresponding to a mean of ∼7% of the mesh covered with satellite wave data at each point. The components of the database generated are the following: longitude (Lon), latitude (Lat), minimum pressure ($P_{\min}$), translation direction (θ_t), translation speed (V_t), and SWH, which will be defined in the congruent mesh discretised by 36 angular sectors of 10° and 10 distances (e.g., Figure 1d).

4 | SOM CLASSIFICATION

Once the database has been generated, the focus is on understanding the wave generation area associated with a tropical cyclone and the effect of the different TC parameters in the shape and magnitude of the waves generated. For this purpose, we use SOMs for clustering combinations of the TC parameters: [$P_{\min}$, V_t, Lat], to later analyse the associated composites of SWH in a 500 km radius area. SOMs are one of the most powerful data mining techniques when clustering high-dimensional data, also due to their visualization properties. The algorithm computes N centroids each characterizing a group of data preserving the topology on its original space. SOMs have been previously applied to evaluate multivariate wave climate (Camus *et al*., 2011a), project changes in synoptic weather patterns (Gibson *et al*., 2016), explore interannual climate variability (Izaguirre *et al*., 2012) among many other applications in the field of the meteorology and oceanography (Liu and Weisberg, 2011).

When comparing the SOM algorithm with other clustering techniques as the maximum dissimilarity analysis (MDA) or the *K*-means clustering (*K*-means), SOM has been ranked the best for the cluster visualization in a 2D lattice (Camus *et al*., 2011b). Nevertheless, it is not the most suitable technique for exploring the boundaries of the data space. For this reason, we have performed a preselection of M = 7,500 points from the full database following MDA to reduce the dimensionality of the full dataset to be further clustered into 49 groups following SOM. To implement the SOM, we use the MiniSom library (Giuseppe, 2019), which is developed in the Python ecosystem. Using this library, we fit the SOM with M, previously selected with MDA, combinations of [$P_{\min}$, V_t, Lat] to obtain 49 clusters. Using the function that determines the Euclidean distance between the data provided and the cluster centroids, a cluster is assigned to every point of the ∼37,000 that compose the database so that every combination of [$P_{\min}$, V_t, Lat] is clustered.

The representation of the centroid of the 49 clusters for the different predictor variables is shown in Figure 2a. A smooth transition between neighbour clusters is observed, facilitating the visual interpretation of the results. Once the predictors are clustered, we analyse the wave data associated to each of the different clusters. The first step is filtering the data outliers at each cell, which have been defined as the SWH values out of the range of the mean ± 4 times the standard deviation. Then, we fit the data in each cell to a generalized extreme value (GEV) distribution, as exemplified in Figure 2g for one selected cluster. To increase the number of data to populate the GEV distribution while smoothing the behaviour between neighbour cells, the distribution is fitted with each cell and its neighbours. The GEV parameters, which are the location (μ), scale (ψ), and the shape (ξ) are shown in Figure 2b–d, respectively. The scale parameter represents the spread of the data, while the mean values of the distribution are defined by

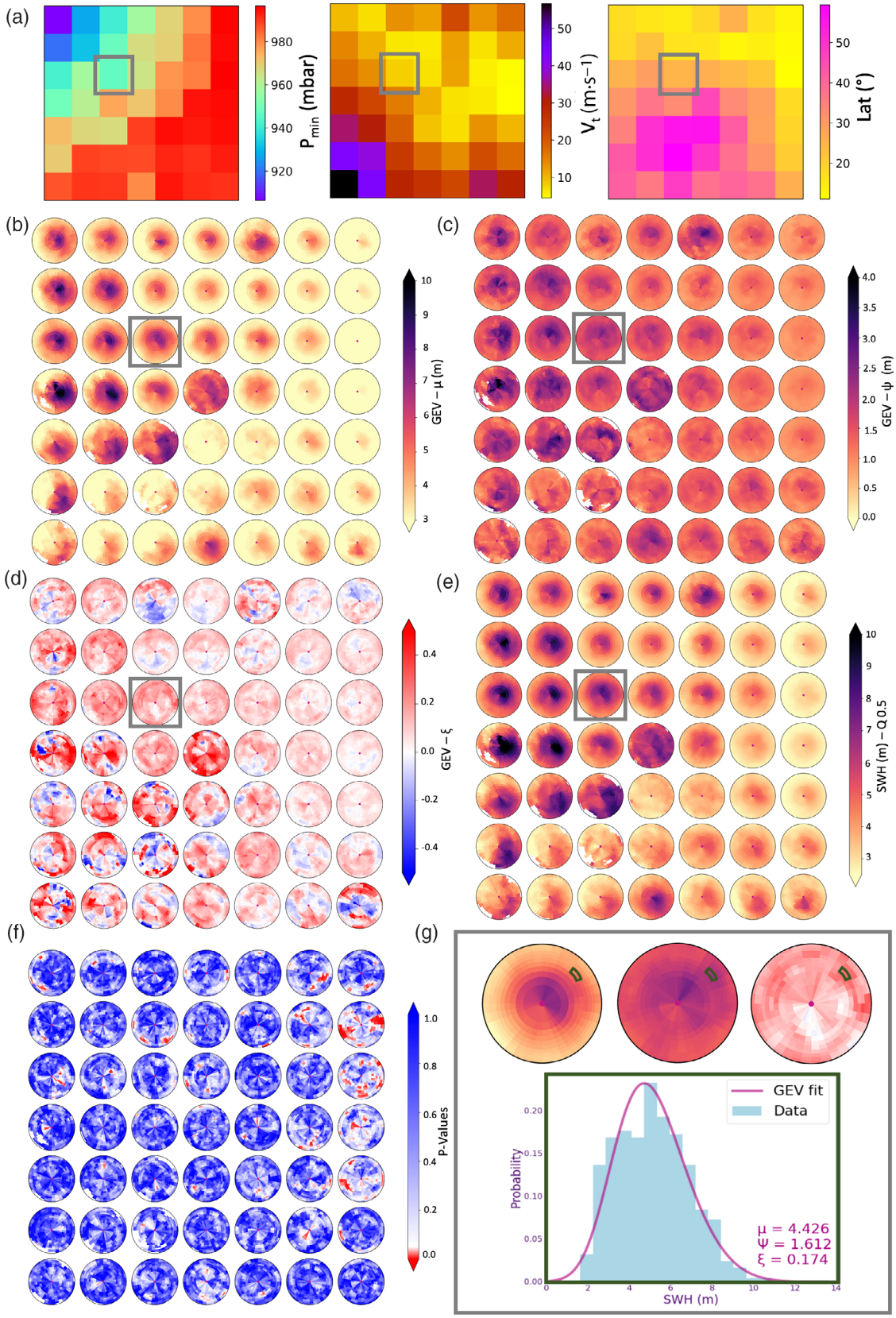

FIGURE 2 SOM classification of the predictors that define the TC characteristics (a). The predictand (SWH) is represented by its fitting to a GEV distribution, defined by μ (b), ψ (c), and ξ (d). As an example, SWH associated to the 0.5 quantile is shown in (e). *p*-values from the Kolmogorov–Smirnov test to estimate the goodness of fit (f) and exemplified obtention of GEV parameters for the highlighted cluster in (a)–(e) and one specific grid cell (g)

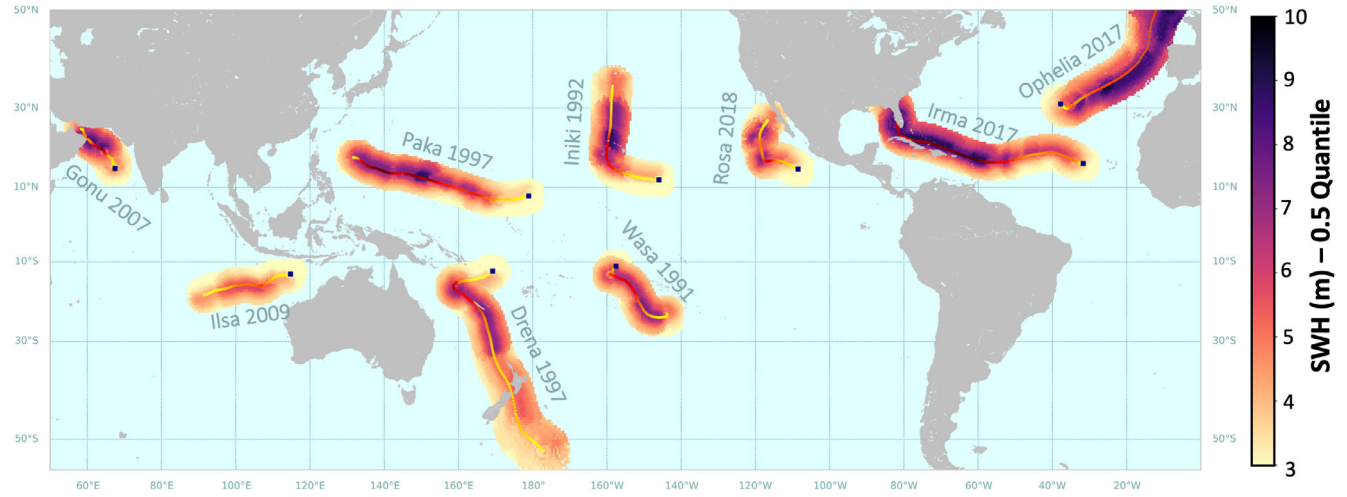

FIGURE 3 Wind wave footprint extracted from the model proposed for a selection of historical TCs worldwide [Colour figure can be viewed at wileyonlinelibrary.com]

the location parameter and the behaviour of the most extreme data is driven by the shape parameter. This last parameter differentiates between Weibull type ($\xi < 0$, blue in Figure 2d), corresponding to a constrained tail of the distribution while, Gumbel type ($\xi = 0$, white in Figure 2d) or Fréchet type ($\xi > 0$, red in Figure 2d) are less constrained, and hence, can extrapolate to larger values.

To estimate the goodness of fit, we perform the Kolmogorov–Smirnov test between the data and the GEV distribution to obtain the *p*-values (Figure 2f) in order to reject the hypothesis that the data comes from the same GEV distribution when the values are below the significance level. Figure 2f shows in red the cells where the p-value is less than 0.05. This occurs at cells where there is a large amount of data, generally associated with less intense TCs. A good general fit to the GEV distribution is present in most of the cells (blues in Figure 2f), and as an example of the magnitude of SWH, Figure 2e shows the 0.5 quantile of the distributions, which pattern is comparable to the location parameter that represents the mean values.

The SOM clustering allows to easily visualize the TC parameters that cause the different composites of SWH. As expected, larger SWHs are mainly associated with low $P_{\min}$ clusters (i.e., more intense TCs), while V_t and Lat allow to characterize the shape of the SWH composite. Largest TCs, in terms of its radius, typically occur at high latitudes (Knaff *et al.*, 2014). The translation speed also plays an important role in the area of influence of a TC. When the translation speed becomes comparable to the group celerity of the waves, waves to the right (left in the SH) of the track are exposed to prolonged wind forcing and a resonance effect is produced (King and Shemdin, 1979; Young, 1988; Moon *et al.*, 2003), referred to as trapped-fetch waves (Bowyer and MacAfee, 2005). When this occurs, the largest values of SWH are produced. For rapidly moving storms (lower left corner cluster in Figure 2) waves generated on the right of the storm are left behind the storm since group velocities are smaller than the translation speed of the storm (Young, 1988). The opposite occurs for slowly moving storms, with waves propagating ahead the storm.

5 | WIND WAVE FOOTPRINT AND VALIDATION AGAINST BUOY DATA

Once the SOM clustering has been developed, the relationships found between the predictors and the SWH composites can be used to derive the SWH from any given TC track just by knowing its representative combinations of [$P_{\min}$, V_t, Lat], θ_t, and the hemisphere. A composite of SWH at each point of the track defines the waves within an area of 500 km radius, and then, the maximum SWH footprint from the TC can be defined as the maximum SWH in a grid discretized every 0.5° both in latitude and longitude.

The outcome of this process is visualized in Figure 3 for a number of TCs worldwide. The figure shows in colour, the maximum SWH at each grid from the composites associated to the 0.5 quantile distribution of the GEV fit (Figure 2e). Also, the track is coloured by its minimum pressure, where darker colours are associated with more intense TCs and the black dot represents the TC genesis.

Wave data from the NDBC buoys represented in Figure 4a are used to validate the historical TCs footprint. For each TC track, buoys within a 500-km buffer are

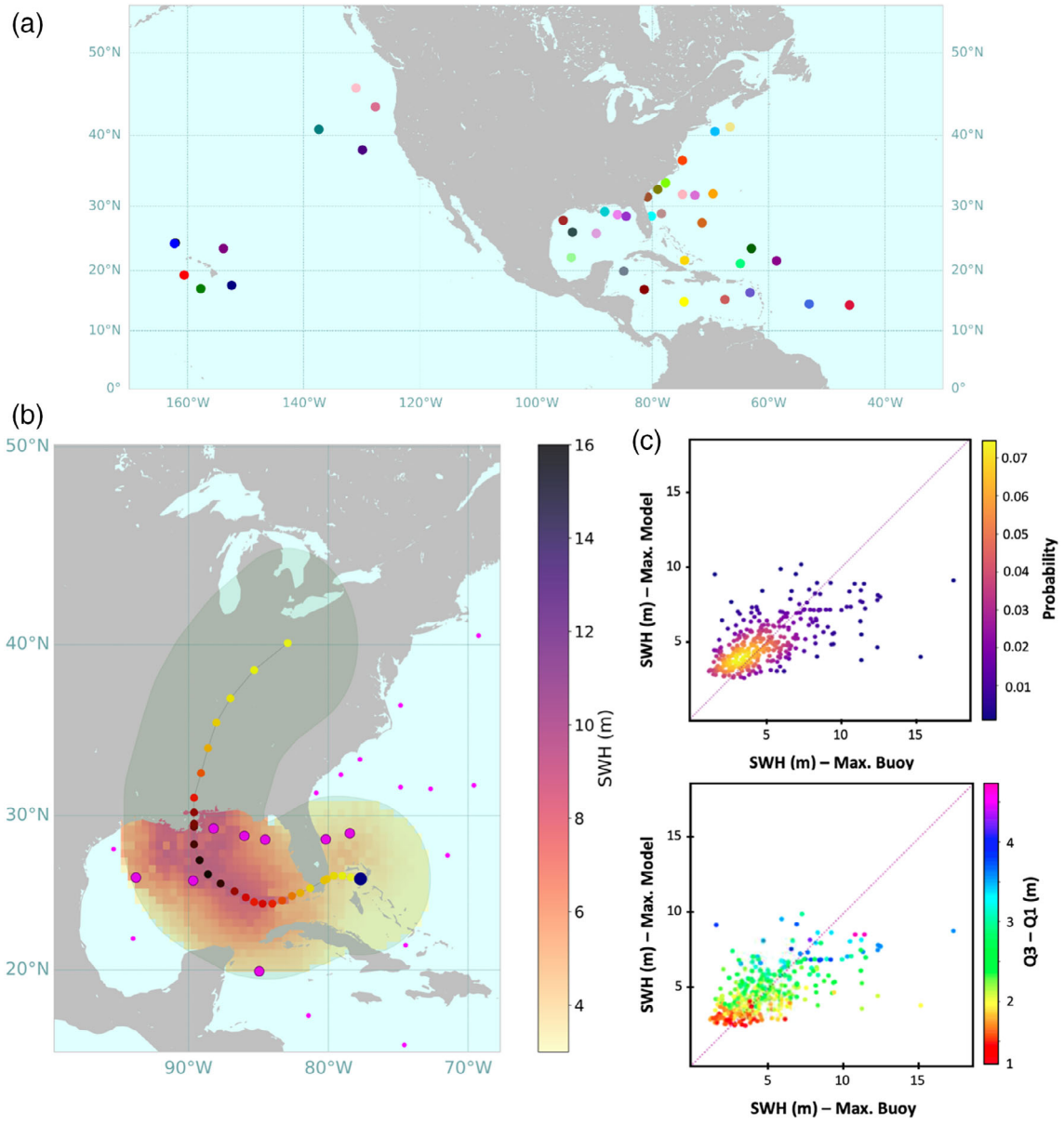

FIGURE 4 Buoy selection and validation. (a) Location of selected NDBC buoys for validation, (b) example of the footprint for a specific TC and the buoys selected in a 500-km buffer (shaded area) from the track (large dots), (c) buoy versus modelled SWH. Colour represents the probability density (d) same as (c), but colour represents the interquartile range [Colour figure can be viewed at wileyonlinelibrary.com]

selected (Figure 4b) and the maximum SWH registered by the buoy against the SWH footprint at the buoy location is compared. Figure 4c represents the scatter of buoy versus modelled SWH associated to the 0.5 quantile of the distributions. The colour refers to the probability density of the scatter, in order to reinforce that most of the values lie on the bisectrix, suggesting that the mean values of the SWH footprint are correctly estimated. Nevertheless, when talking about very large extremes, the percentile 0.5 of the GEV distribution does not capture waves up to 16 m, caused by extreme TCs as Katrina in 2005 (Wang and Oey, 2008) probably because the number of data to populate those bins associated with extreme events is not large enough. Figure 4d represents the interquartile range of the fit, which increases with the SWH, and reaches up to 4.8 m for some extreme estimations, which is too large to give a confident estimate of these values.

Although the database generated aggregates all the historical combinations of TCs and satellite wave data, a larger dataset will be required to capture and populate all the plausible combinations (Tamizi and

Young, 2020). This is even more relevant when trying to explain the most extreme waves. This model can be used to understand the distribution of SWH within a TC track and, at a low computational expense, to provide a first order estimate. Nevertheless, it is important to understand that although the spatial distribution of SWH may correctly reflect the waves generated by a TC and its mean value, very extreme events are likely to be underpredicted, a problem common to parametric modelling (e.g., Young, 2017).

6 | SUMMARY AND CONCLUSIONS

This work presents a comprehensive dataset with over a million satellite observations of waves under the influence of historical TCs worldwide. The database has been analysed using an efficient clustering technique (SOM) that allows to explore in an easy to understand 2D lattice, the influence of different TC predictors, as the minimum pressure, the translation speed, and the latitude, in the shape and magnitude of the SWH generated. Taking advantage of the full dimensionality of the data, the results show a clear pattern in how the different TC parameters relate to the SWH. It is found that the pressure is the main driver for the larger wave heights, while the size of the SWH footprint is explained by the latitude, being the larger TCs the ones located at higher latitudes. The translation speed explains whether the larger waves are left behind or travel ahead the storm depending on whether the speed is larger or smaller than the group velocity respectively.

Besides the properties of the SOM analysis to improve the understanding of the SWH field generated, the composites can be used to derive a first estimation of the SWH footprint of any historical or synthetic TC worldwide, although the accuracy of the most extreme events is at the moment limited. Although in this work, and in order to find a balance between the number of clusters and the data to populate each of them, the number of clusters has been set up to 49, a larger number of groups will improve the characterization of these extreme events. This is something that could easily be done in the future taking advantage of the rapidly increasing amount of altimeter data that is being produced worldwide.

To make the model accessible to the community, we have created a GitLab repository with the codes to derive the SWH footprint for any historical TC from the IBTrACS dataset, with the potential to be adapted to any other TC synthetic database. The codes, which have been developed in the Python language under the Jupyter Notebook ecosystem, and all the necessary data for them to be run can be accessed and downloaded from https://gitlab.com/geoocean/bluemath/tcs/wave-footprint-satellite. As an estimation of the SWH footprint associated to a TC can be derived in a matter of seconds, we believe this tool can be of great interest for supporting risk assessments or early warning systems worldwide.

ACKNOWLEDGEMENTS

This work would not have been possible without funding from the Strategic Environmental Research and Development Program's grant DOD/SERDP RC-2644 and from the Spanish Ministry of Science and Innovation, project Beach4cast PID2019-107053RB-I00. Ana Rueda funded by a Juan de la Cierva Incorporación Scholarship (IJC2020-04390). Laura Cagigal is funded by a scholarship from the University of Auckland. Open access publishing facilitated by The University of Auckland, as part of the Wiley - The University of Auckland agreement via the Council of Australian University Librarians.

DATA AVAILABILITY STATEMENT

Tropical Cyclone Data from IBTrACS can be downloaded from https://www.ncei.noaa.gov/data/international-best-track-archive-for-climate-stewardship-ibtracs/v04r00/access/netcdf/, IMOS database can be accessed from https://doi.org/10.26198/5c77588b32cc1.

ORCID

Laura Cagigal https://orcid.org/0000-0001-5384-6382
Fernando J. Méndez https://orcid.org/0000-0002-5005-1100
Sara O. van Vloten https://orcid.org/0000-0001-7832-955X
Ana Rueda https://orcid.org/0000-0001-9383-4861
Giovanni Coco https://orcid.org/0000-0001-7435-1602

REFERENCES

Abdalla, S., Abdeh Kolahchi, A., Ablain, M., Adusumilli, S., Aich Bhowmick, S., Alou-Font, E., Amarouche, L., Andersen, O.B., Antich, H., Aouf, L., Arbic, B., Armitage, T., Arnault, S., Artana, C., Aulicino, G., Ayoub, N., Badulin, S., Baker, S., Banks, C., Bao, L., Barbetta, S., Barceló-Llull, B., Barlier, F., Basu, S., Bauer-Gottwein, P., Becker, M., Beckley, B., Bellefond, N., Belonenko, T., Benkiran, M., Benkouider, T., Bennartz, R., Benveniste, J., Bercher, N., Berge-Nguyen, M., Bettencourt, J., Blarel, F., Blazquez, A., Blumstein, D., Bonnefond, P., Borde, F., Bouffard, J., Boy, F., Boy, J.P., Brachet, C., Brasseur, P., Braun, A., Brocca, L., Brockley, D., Brodeau, L., Brown, S., Bruinsma, S., Bulczak, A., Buzzard, S., Cahill, M., Calmant, S., Calzas, M., Camici, S., Cancet, M., Capdeville, H., Carabajal, C.C., Carrere, L., Cazenave, A., Chassignet, E.P., Chauhan, P., Cherchali, S., Chereskin, T., Cheymol, C., Ciani, D., Cipollini, P., Cirillo, F., Cosme, E., Coss, S., Cotroneo, Y., Cotton, D., Couhert, A., Coutin-Faye, S.,

Crétaux, J.F., Cyr, F., d'Ovidio, F., Darrozes, J., David, C., Dayoub, N., de Staerke, D., Deng, X., Desai, S., Desjonqueres, J. D., Dettmering, D., di Bella, A., Díaz-Barroso, L., Dibarboure, G., Dieng, H.B., Dinardo, S., Dobslaw, H., Dodet, G., Doglioli, A., Domeneghetti, A., Donahue, D., Dong, S., Donlon, C., Dorandeu, J., Drezen, C., Drinkwater, M., du Penhoat, Y., Dushaw, B., Egido, A., Erofeeva, S., Escudier, P., Esselborn, S., Exertier, P., Fablet, R., Falco, C., Farrell, S.L., Faugere, Y., Femenias, P., Fenoglio, L., Fernandes, J., Fernández, J.G., Ferrage, P., Ferrari, R., Fichen, L., Filippucci, P., Flampouris, S., Fleury, S., Fornari, M., Forsberg, R., Frappart, F., Frery, M.L., Garcia, P., Garcia-Mondejar, A., Gaudelli, J., Gaultier, L., Getirana, A., Gibert, F., Gil, A., Gilbert, L., Gille, S., Giulicchi, L., Gómez-Enri, J., Gómez-Navarro, L., Gommenginger, C., Gourdeau, L., Griffin, D., Groh, A., Guerin, A., Guerrero, R., Guinle, T., Gupta, P., Gutknecht, B.D., Hamon, M., Han, G., Hauser, D., Helm, V., Hendricks, S., Hernandez, F., Hogg, A., Horwath, M., Idžanović, M., Janssen, P., Jeansou, E., Jia, Y., Jia, Y., Jiang, L., Johannessen, J.A., Kamachi, M., Karimova, S., Kelly, K., Kim, S.Y., King, R., Kittel, C.M.M., Klein, P., Klos, A., Knudsen, P., Koenig, R., Kostianoy, A., Kouraev, A., Kumar, R., Labroue, S., Lago, L.S., Lambin, J., Lasson, L., Laurain, O., Laxenaire, R., Lázaro, C., le Gac, S., le Sommer, J., le Traon, P.Y., Lebedev, S., Léger, F., Legresy, B. ˆ., Lemoine, F., Lenain, L., Leuliette, E., Levy, M., Lillibridge, J., Liu, J., Llovel, W., Lyard, F., Macintosh, C., Makhoul Varona, E., Manfredi, C., Marin, F., Mason, E., Massari, C., Mavrocordatos, C., Maximenko, N., McMillan, M., Medina, T., Melet, A., Meloni, M., Mertikas, S., Metref, S., Meyssignac, B., Minster, J.F., Moreau, T., Moreira, D., Morel, Y., Morrow, R., Moyard, J., Mulet, S., Naeije, M., Nerem, R.S., Ngodock, H., Nielsen, K., Nilsen, J.E.Ø., Niño, F., Nogueira Loddo, C., Noûs, C., Obligis, E., Otosaka, I., Otten, M., Oztunali Ozbahceci, B., P. Raj, R., Paiva, R., Paniagua, G., Paolo, F., Paris, A., Pascual, A., Passaro, M., Paul, S., Pavelsky, T., Pearson, C., Penduff, T., Peng, F., Perosanz, F., Picot, N., Piras, F., Poggiali, V., Poirier, É., Ponce de León, S., Prants, S., Prigent, C., Provost, C., Pujol, M.I., Qiu, B., Quilfen, Y., Rami, A., Raney, R.K., Raynal, M., Remy, E., Rémy, F., Restano, M., Richardson, A., Richardson, D., Ricker, R., Ricko, M., Rinne, E., Rose, S.K., Rosmorduc, V., Rudenko, S., Ruiz, S., Ryan, B.J., Salaün, C., Sanchez-Roman, A., Sandberg Sørensen, L., Sandwell, D., Saraceno, M., Scagliola, M., Schaeffer, P., Scharffenberg, M.G., Scharroo, R., Schiller, A., Schneider, R., Schwatke, C., Scozzari, A., Ser-giacomi, E., Seyler, F., Shah, R., Sharma, R., Shaw, A., Shepherd, A., Shriver, J., Shum, C.K., Simons, W., Simonsen, S.B., Slater, T., Smith, W., Soares, S., Sokolovskiy, M., Soudarin, L., Spatar, C., Speich, S., Srinivasan, M., Srokosz, M., Stanev, E., Staneva, J., Steunou, N., Stroeve, J., Su, B., Sulistioadi, Y.B., Swain, D., Sylvestre-baron, A., Taburet, N., Tailleux, R., Takayama, K., Tapley, B., Tarpanelli, A., Tavernier, G., Testut, L., Thakur, P. K., Thibaut, P., Thompson, L.A., Tintoré, J., Tison, C., Tourain, C., Tournadre, J., Townsend, B., Tran, N., Trilles, S., Tsamados, M., Tseng, K.H., Ubelmann, C., Uebbing, B., Vergara, O., Verron, J., Vieira, T., Vignudelli, S., Vinogradova Shiffer, N., Visser, P., Vivier, F., Volkov, D., von Schuckmann, K., Vuglinskii, V., Vuilleumier, P., Walter, B., Wang, J., Wang, C., Watson, C., Wilkin, J., Willis, J., Wilson, H., Woodworth, P., Yang, K., Yao, F., Zaharia, R., Zakharova, E., Zaron, E.D., Zhang, Y., Zhao, Z., Zinchenko, V. and Zlotnicki, V. (2021) Altimetry for the future: building on 25 years of progress. *Advances in Space Research*, 68(2), 319–363. https://doi.org/10.1016/j.asr.2021.01.022.

Beckers, B. and Beckers, P. (2012) A general rule for disk and hemisphere partition into equal-area cells. *Computational Geometry: Theory and Applications*, 45(7), 275–283. https://doi.org/10.1016/j.comgeo.2012.01.011.

Bloemendaal, N., Haigh, I.D., de Moel, H., Muis, S., Haarsma, R.J. and Aerts, J.C.J.H. (2020) Generation of a global synthetic tropical cyclone hazard dataset using STORM. *Scientific Data*, 7(1), 1–12. https://doi.org/10.1038/s41597-020-0381-2.

Bowyer, P.J. and MacAfee, A.W. (2005) The theory of trapped-fetch waves with tropical cyclones—an operational perspective. *Weather and Forecasting*, 20(3), 229–244. https://doi.org/10.1175/WAF849.1.

Cagigal, L., Rueda, A., Castanedo, S., Cid, A., Perez, J., Stephens, S. A., Coco, G. and Méndez, F.J. (2019) Historical and future storm surge around New Zealand: from the 19th century to the end of the 21st century. *International Journal of Climatology*, 40(3), 1512–1525. https://doi.org/10.1002/joc.6283.

Camus, P., Cofiño, A.S., Mendez, F.J. and Medina, R. (2011a) Multivariate wave climate using self-organizing maps. *Journal of Atmospheric and Oceanic Technology*, 28(11), 1554–1568. https://doi.org/10.1175/JTECH-D-11-00027.1.

Camus, P., Mendez, F.J., Medina, R. and Cofiño, A.S. (2011b) Analysis of clustering and selection algorithms for the study of multivariate wave climate. *Coastal Engineering*, 58(6), 453–462. https://doi.org/10.1016/j.coastaleng.2011.02.003.

Cid, A., Camus, P., Castanedo, S., Méndez, F.J. and Medina, R. (2017) Global reconstructed daily surge levels from the 20th century reanalysis (1871–2010). *Global and Planetary Change*, 148, 9–21. https://doi.org/10.1016/j.gloplacha.2016.11.006.

Daloz, A.S. and Camargo, S.J. (2018) Is the poleward migration of tropical cyclone maximum intensity associated with a poleward migration of tropical cyclone genesis? *Climate Dynamics*, 50(1–2), 705–715. https://doi.org/10.1007/s00382-017-3636-7.

Durrant, T., Greenslade, D., Hemar, M. and Trenham, C. (2014) A Global Hindcast focussed on the central and South Pacific. CAWCR technical report.

Emanuel, K.A. (2013) Downscaling CMIP5 climate models shows increased tropical cyclone activity over the 21st century. *Proceedings of the National Academy of Sciences of the United States of America*, 110(30), 12219–12224. https://doi.org/10.1073/pnas.1301293110.

Gibson, P.B., Perkins-Kirkpatrick, S.E. and Renwick, J.A. (2016) Projected changes in synoptic weather patterns over New Zealand examined through self-organizing maps. *International Journal of Climatology*, 36(12), 3934–3948. https://doi.org/10.1002/joc.4604.

Giuseppe Vettigli. (2019). MiniSom: minimalistic and NumPybased implementation of the Self Organizing Map. Release 2.1.5. https://github.com/JustGlowing/minisom

Hemer, M.A., Fan, Y., Mori, N., Semedo, A. and Wang, X.L. (2013) Projected changes in wave climate from a multi-model ensemble. *Nature Climate Change*, 3(5), 471–476. https://doi.org/10.1038/nclimate1791.

Hodges, K., Cobb, A. and Vidale, P.L. (2017) How well are tropical cyclones represented in reanalysis datasets? *Journal of Climate*, 30(14), 5243–5264. https://doi.org/10.1175/JCLI-D-16-0557.1.

Hoeke, R.K., Damlamian, H., Aucan, J. and Wandres, M. (2021) Severe flooding in the atoll nations of Tuvalu and Kiribati triggered by a distant tropical cyclone pam. *Frontiers in Marine Science*, 7, 1–12. https://doi.org/10.3389/fmars.2020.539646.

Hoogewind, K.A., Chavas, D.R., Schenkel, B.A. and O'Neill, M.E. (2020) Exploring controls on tropical cyclone count through the geography of environmental favorability. *Journal of Climate*, 33(5), 1725–1745. https://doi.org/10.1175/JCLI-D-18-0862.1.

Izaguirre, C., Menéndez, M., Camus, P., Méndez, F.J., Mínguez, R. and Losada, I.J. (2012) Exploring the interannual variability of extreme wave climate in the Northeast Atlantic Ocean. *Ocean Modelling*, 59–60, 31–40. https://doi.org/10.1016/j.ocemod.2012.09.007.

King, D.B. and Shemdin, O.H. (1979) Radar observations of hurricane wave directions. *Proceedings of the Coastal Engineering Conference*, 1, 209–226. https://doi.org/10.9753/icce.v16.10.

Kita, Y., Waseda, T. and Webb, A. (2018) Development of waves under explosive cyclones in the northwestern Pacific. *Ocean Dynamics*, 68(10), 1403–1418. https://doi.org/10.1007/s10236-018-1195-z.

Knaff, J.A., Longmore, S.P. and Molenar, D.A. (2014) An objective satellite-based tropical cyclone size climatology. *Journal of Climate*, 27(1), 455–476. https://doi.org/10.1175/JCLI-D-13-00096.1.

Knapp, K.R., Diamond, H.J., Kossin, J.P., Kruk, M.C. and Schreck, C.J. (2018) *International Best Track Archive for Climate Stewardship (IBTrACS) Project, Version 4*. NOAA National Centers for Environmental Information. https://doi.org/10.25921/82ty-9e16.

Liu, Y. and Weisberg, R.H. (2011) A review of self-organizing map applications in meteorology and oceanography. In: J. I. Mwasiagi, Ed., *Self-Organizing Maps: Applications and Novel Algorithm Design*, InTech, pp. 253–272.

Moon, I.-J., Hara, T., Tolman, H.L., Wright, C.W. and Walsh, E.J. (2003) Numerical simulation of sea surface directional wave spectra under typhoon wind forcing. *Journal of Hydrodynamics*, 33, 1680–1706. https://doi.org/10.1016/S1001-6058(09)60015-9.

Mori, N. and Takemi, T. (2016) Impact assessment of coastal hazards due to future changes of tropical cyclones in the North Pacific Ocean. *Weather and Climate Extremes*, 11, 53–69. https://doi.org/10.1016/j.wace.2015.09.002.

Ponce de León, S. and Bettencourt, J.H. (2021) Composite analysis of North Atlantic extra-tropical cyclone waves from satellite altimetry observations. *Advances in Space Research*, 68(2), 762–772. https://doi.org/10.1016/j.asr.2019.07.021.

Ribal, A. and Young, I.R. (2019) 33 years of globally calibrated wave height and wind speed data based on altimeter observations. *Scientific Data*, 6(1), 1–15. https://doi.org/10.1038/s41597-019-0083-9.

Takbash, A., Young, I.R. and Breivik, Ø. (2019) Global wind speed and wave height extremes derived from long-duration satellite records. *Journal of Climate*, 32(1), 109–126. https://doi.org/10.1175/JCLI-D-18-0520.1.

Tamizi, A. and Young, I.R. (2020) The spatial distribution of ocean waves in tropical cyclones. *Journal of Physical Oceanography*, 50(8), 2123–2139. https://doi.org/10.1175/JPO-D-20-0020.1.

Walsh, K.J.E., McInnes, K.L. and McBride, J.L. (2012) Climate change impacts on tropical cyclones and extreme sea levels in the South Pacific—a regional assessment. *Global and Planetary Change*, 80–81, 149–164. https://doi.org/10.1016/j.gloplacha.2011.10.006.

Wang, D.-P. and Oey, L.-Y. (2008) Hindcast of waves and currents in Hurricane Katrina. *Bulletin of the American Meteorological Society*, 89, 487–495.

Young, I.R. and Vinoth, J. (2013) An "extended fetch" model for the spatial distribution of tropical cyclone wind-waves as observed by altimeter. *Ocean Engineering*, 70, 14–24. https://doi.org/10.1016/j.oceaneng.2013.05.015.

Young, I.R. (1988) Parmatric hurricane wave prediction model. *Journal of Waterway, Port, Coastal and Ocean Engineering*, 114(5), 637–652.

Young, I.R. (2017) A review of parametric descriptions of tropical cyclone wind-wave generation. *Atmosphere*, 8(10), 194. https://doi.org/10.3390/atmos8100194.

How to cite this article: Cagigal, L., Méndez, F. J., van Vloten, S. O., Rueda, A., & Coco, G. (2022). Wind wave footprint of tropical cyclones from satellite data. *International Journal of Climatology*, 1–10. https://doi.org/10.1002/joc.7764